Structures 23 (2020) 304–313

Contents lists available at ScienceDirect

Structures

journal homepage: www.elsevier.com/locate/structures

Effect of compressive strength of concrete on transmission length of pre-tensioned concrete systems

Prabha Mohandoss, Radhakrishna G. Pillai*, Amlan K. Sengupta

Department of Civil Engineering, Indian Institute of Technology Madras, Chennai, India

ARTICLE INFO

Keywords:
Bond
Prestressed
Pretensioned concrete
Strand
Transmission length

ABSTRACT

This paper presents an experimental study on L_t in pre-tensioned concrete (PTC) members made of four values of compressive strength of concrete. Also, it presents a comparison between the formulations of transmission length (L_t) given in various codes and other literature. A test specimen consisted of a concrete prism (100 × 100 × 2000) mm with a prestressed seven–wire strand (12.7 mm diameter) at the center. The values of average compressive strength for concrete at transfer (f_{ci}) were 23, 28, 36, and 43 MPa. The challenges involved with the measurements of DEMEC readings, difference between the readings from surface–mounted discs and the inserts are discussed. The results indicate that L_t could decrease by 33% when the f_{ci} increases from about 23 to 43 MPa. Based on this data, a new bi-linear formulation to determine the L_t as a function of f_{ci} is proposed. Further, it is shown that higher estimates of L_t as per the available formulations, will lead to lower estimate of bursting tensile stress in concrete generated during transfer. Hence, a precise estimate of L_t as a function of the strength of concrete at transfer is expected to provide more rational design of transmission zone reinforcement.

1. Introduction

Pre-tensioned concrete (PTC) elements with seven-wire strands are widely used in many structures. The length required to transfer the prestress (f_{pe}) from strand to concrete is defined as the transmission length (L_t). Fig. 1 shows the schematic variations of stress and strain along the length of a strand at the stage of transfer of prestress. As shown by Line 1 (in Fig. 1(a)), the stress at the end of the member is zero (at $x = 0, f_{ps} = 0$), the stress gradually increases to the prestress at transfer f_{pe}, and then remains constant in absence of external load (as depicted by Line 2, at $x = L_t, f_{ps} = f_{pe}$). Similarly, the strain in the strand and axial strain in concrete varies along L_t (Fig. 1(b)). Typically, the shear demand in the transmission zone (say, near support regions) of a simply supported PTC element systems is high. Therefore, if prestress is not transferred adequately within the desired distance from the end of the member, the shear critical sections near the support may experience shear failure. Fig. 2 shows an example of the shear cracks observed in the end regions near the support on highway bridge girders. Such shear cracks could occur due to the poor construction practices leading to inadequate compressive strength or bond strength of concrete, inadequate amount of stirrups and inadequate design expression for L_t. Some codal provisions adopt empirical formulations based on the diameter of strand and do not consider the various properties of concrete to estimate L_t. This may result in less conservative or less rational shear design near the supports [1,2]. Hence, more rational formulations, by incorporating the properties of both strand and concrete, and the prestress level must be developed to determine L_t. A previous paper addressed the importance of determining L_t precisely and the details of the experimental programme conducted [3].

This paper presents the analysis of the experimental data, to study the effect of compressive strength of concrete at transfer (f_{ci}) on L_t. A bi–linear formulation of L_t with respect to f_{ci} was developed. The values of L_t from the proposed model were compared with those estimated using IS 1343 (2012), ACI 318 (2014), AASHTO LFRD (2012), AS 3600 (2009), and CSA A23 (2004) codes. Also, an example pre-tensioned girder was studied to investigate the effect of over-estimation of L_t on the estimation of bursting tensile stress in the transmission zone.

1.1. Mechanism of strand–concrete bond

The S–C bond is mainly governed by the adhesion, friction, and mechanical interlock mechanisms [4,5]. Adhesion plays a minimal role in transferring the prestress as the slipping of the strand with respect to the hardened concrete during the stress transfer can destroy the adhesive bond [1]. The friction is developed by the Hoyer effect of the

* Corresponding author.
E-mail address: pillai@iitm.ac.in (R.G. Pillai).

https://doi.org/10.1016/j.istruc.2019.09.016
Received 22 August 2019; Received in revised form 16 September 2019; Accepted 17 September 2019
Available online 04 December 2019

Nomenclature

α	Proportionality constant and coefficient used in the L_t equation by Barnes et al. (2003) and Pellegrino et al. (2016)
$\alpha 1$	Factor to account the releasing method
$\alpha 2$	Factor to account the type of strand in EN 2 (2004) and the action effect in *fib*-MC (2010)
$\alpha 3$	Factor for pretensioned strand in *fib*–MC (2010)
β, γ, δ	Coefficient used in the L_t equation Pellegrino et al. (2016)
λ	Factor to account for the concrete type
$\Delta\varepsilon_p$	Strain difference in prestressed strands
Δl	Change in distance (mm)
K_t	Factor to account the type of tendon in BS 8110 (1997)
d_s	Diameter of the prestressing strand (mm)
$\varepsilon_{c(x)}$	Strain on the concrete surface at x distance
$\varepsilon'_{c(x)}$	Smoothened strain on the concrete surface at x distance
ε_{ce}	Effective strain on the concrete surface
ε_{pe}	Effective strain in prestressing strands
b_w	Width of the cross section at the centroid (mm)
f_{bpt}	Bond stress at the time of releasing (MPa)
f_{ci}	Compressive strength of concrete at time of prestress transfer (MPa)
f_{ctd}	Design tensile strength of concrete (MPa)
f_{pe}	Effective stress in prestressing steel after allowance for all losses (MPa)
f_{pi}	Initial prestress of the strand (MPa)
f_{pk}	Characteristic tensile stress in strand (MPa)
f_s	Permissible stress in the reinforcement (MPa)
f_v	Transverse tensile stress at the centroid of the end face (MPa)
f_t	Tensile stress (MPa)
k_1	Factor to account for the distance of section considered from L_t
l_x	Distance of section considered from the starting point of the L_t(mm)
p	Perimeter of the strand (mm)
A	Cross-sectional area of the concrete (mm^2)
A_{ps}	Circumferential area of the strand (mm^2)
A_{sv}	Area of vertical steel required (mm^2)
D	Overall depth of the member (mm)
$Fbat$	Transverse tensile force (kN)
L_t	Transmission length (mm)
$L_{t,\ code}$	Calculated L_t using codal formulations (mm)
$L_{t,\ measured}$	Experimentally obtained L_t (mm)
$L_{t,\ estimated}$	Estimated L_t based on proposed model (mm)
M	Initial moment due to prestress (N mm)

strand and confinement of concrete. During prestressing, the strand is elongated and when the prestress is transferred to the surrounding hardened concrete, the strand tries to shorten longitudinally and expand laterally due to Poisson's effect. However, the surrounding confined concrete provides wedge action and induces compressive stresses perpendicular to the S-C interface. This increases the frictional force,

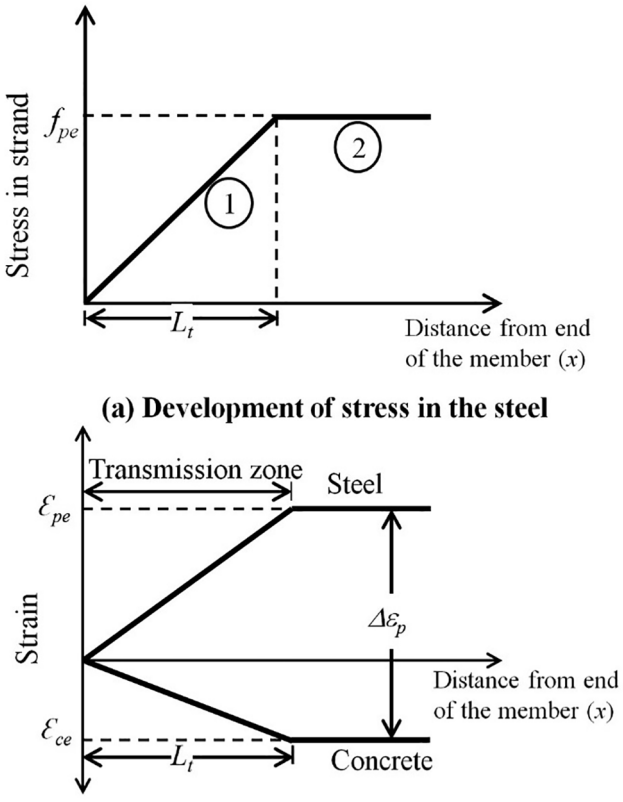

Fig. 1. Schematic diagrams showing idealized variation of stresses and strains.

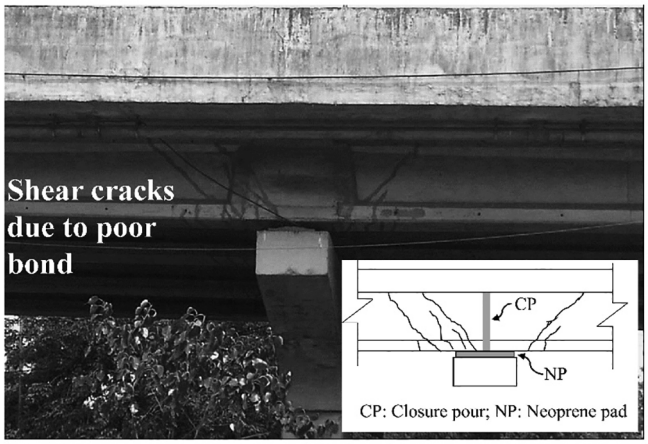

Fig. 2. Shear cracks in a highway bridge girder.

which in turn enhances the bond. This phenomenon is known as the Hoyer effect [6]. In addition, the mechanical interlock occurs due to the bearing stress provided by the grooves formed by the outer helically twisted wires.

1.2. Factors affecting L_t

The L_t of PTC members is highly dependent on the concrete and strand properties and amount and method of prestressing operations. The diameter of the strand (d_s), the surface conditions of the strand, the compressive strength of concrete at transfer (f_{ci}), the confinement due to the presence of closed stirrups, the method of prestress transfer (gradual or sudden), and other time–dependent effects (creep and shrinkage) can affect the L_t in PTC members. These factors affecting the L_t could be classified into two broad categories: (i) strand and associated properties and (ii) concrete and associated properties.

1.2.1. Strand and associated properties

The cross-sectional geometry of the strand determines the available surface area to be bonded with the concrete to transfer the prestress.

The AASHTO LRFD (2012), ACI 318 (2014), AS 3600 (2009), CSA 23 (2014), EN 2 (2004), IRC 112 (2011), *fib*–MC (2010), and IS 1343 (2012) codes consider this in an empirical way – by using the diameter of the strand (d_s) and a multiplier in the equation for L_t [7–14]. It is to be noted that, the pitch of the helical outer wires influences the S–C bond mechanism – longer the pitch, the lesser will be the angle between the outer and center wires – leading to lower bearing and mechanical interlock provided. Surface condition of the strand is also critical to be considered as it influences the adhesion and frictional mechanisms of S–C bond. Rough or indented surface can enhance the friction and reduce the L_t [1,15,16].

The method of prestressing can also influence the L_t. The gradual and sudden methods of transfer of prestress can have different dynamics of energy at stress transfer [17,18]. In a sudden release of the stretched strand, the end portion of the strand does not get enough time to transmit the energy – resulting in longer L_t than that achieved in a gradual release method [1,19]. Russell and Burns (1997) also reported that the effect due to the releasing method becomes less significant as the length of the PTC element increases [20]. However, the gradual release method is recommended and it is followed in the current study.

1.2.2. Concrete and associated properties

Based on the studies using low strength concretes prevailing in the 1950s, Hanson and Kaar (1959) found no relationship between L_t and f_{ci} – similar to some of the findings in this paper [5]. However, several studies after that indicated that the L_t decreases with increase in f_{ci} [1,16,21–27]. Details on these studies and comparing their results are provided later in this paper. The concrete composition – the amount of cement and water–cement ratio used could also influence the L_t as they primarily contribute to the strength development [28]. However, some researchers reported no significant change in L_t with different type of concrete due to relatively small specimen size, especially between the self-consolidated concrete and conventional concrete [29–30]. The stiffness and confinement of concrete, and their effects on L_t tend to increase as the concrete strength at transfer is higher, which in turn results in increased friction and shorter L_t [1,28,31]. In addition to the lateral confinement provided by the concrete matrix, the closed stirrups also provide confinement. Russell and Burns (1996) and Kim et al. (2016) reported that the effect of stirrups on L_t is negligible [32,33]. On the other hand, Vázquez-Herrero et al., 2013 reported that it could help to minimize variations in L_t as a function of time – in laboratory studies [34]. It should be noted that considering size effect, correlating the L_t of laboratory specimens with single-strand and a few stirrups with that of structural elements with multi-strands and many stirrups is challenging and is not a focus of the current study.

As the maturity of concrete continues to increase with curing, the S–C bond improves. This, in long term, could help in counteracting the possible adverse effects such as loss of prestress due to creep, shrinkage, and relaxation [35–37]. One reviewed literature did not reveal any consistent information on the systematic variation of L_t with time. For example, reported findings say that L_t can increase or decrease or may not change with time – as it depends on many other external conditions [1,23,38–41]. Thus, the time-dependent effects on L_t for concretes with different compressive strengths are not well-reported/modelled in literature.

1.3. L_t equations provided in the codes and literature

Table 1 provides the design L_t equations from the codes and literature studied and Table 2 summarizes the different parameters considered in the codes. In this paper, L_t calculated using various codal equations is denoted as $L_{t,\ code}$. ACI 318 (2014), AASHTO LFRD (2012), AS 3600 (2009), CSA A23 (2004), and IS 1343 (2012) provide empirical equations with d_s as the only variable. The formula given in ACI 318 (2014) are based on the experimental work by Hanson and Kaar (1959). In this, the denominator '20.7' represents the f_{ck} of typical concrete used in the 1950s [21]. However, the properties of concrete and steel used today are different; hence, for a more rational design, such equations need to be modified to reflect the properties of today's concrete and steel. BS 8110 (1997) code considers d_s and f_{ci} and not f_{pe} [42]. Later, this code became obsolete and the EN 2 specifications was adopted in general practice.

EN 2 (2004) and *fib*-MC (2010) consider f_{ci} to compute the bond stress. Considering the bond stress or S-C interface condition could result in a better estimation of L_t [43]. Both EN 2(2004) and *fib*–MC (2010) considered many factors to account for the effect of prestress releasing method, type of strand, structural action (flexural/shear), and position/profile of the strand. Both these codes consider upper and lower bound values for L_t to verify the design. EN 2 (2004) considers 0.8 and 1.2 times L_t as its lower and upper bound values to check local stresses at prestress transfer and ultimate limit states, respectively. On the other hand, *fib*-MC (2010) considers factor of 0.5 and 1 as lower and upper bound values for L_t to check the design. ACI 318 (2014), AASHTO LFRD (2012), AS 3600 (2009), and IS 1343 (2012) do not suggest upper/lower bound values to check the design at transfer and ultimate. In this case, the calculated L_t using these codes could significantly influence the structural performance of PTC systems. The IRC 112 (2011) has adopted the approach of EN 2 (2004). However, the suggested assumptions/values on these factors could be questionable. More work needs to be done in this area and is out of the scope of the current work.

Shahawy et al. (1992), Deatherage et al. (1994), and Bucker (1995) suggested L_t equations with f_{pi} as a variable and not f_{ci} (similar to ACI 318) [44–46]. On the other hand, Zia and Moustafa (1977), Cousins et al. (1990), Mitchell et al. (1993), Lane (1998), Barnes et al. (2003), Martí-Vargas et al. (2006), Kose and Burkett (2007), Ramirez and Russell (2008), Pellegrino et al. (2015), and Ramirez–Garcia et al. (2016) proposed different L_t equations with f_{ci} as a variable [1,16,21–24,26–28,47,48].

To understand the effect of f_{ci} on L_t, about 200 experimental data

Table 1
Equations for L_t in the studied literature.

Equation for L_t	Sources
Codes	
$\frac{f_{pe}}{20.7}d_s$	ACI-318 (1963–2014)
$60d_s$	AASHTO LFRD (2012) & AS 3600 (2009)
$50d_s$	CSA A23 (2004)
$30d_s$	IS 1343 (2012)
$\frac{K_t d_s}{\sqrt{f_{ci}}}$	BS 8110 (1997)
$\alpha_1\alpha_2\frac{f_{pi}}{f_{bpt}}d_s$	EN 2 (2004), IRC:112 (2011)
$\alpha_1\alpha_2\alpha_3\frac{f_{pi}}{f_{bpt}}\frac{A_{ps}}{\pi d_s}$	*fib* MC (2010)
Research studies	
$80d_s$	Martin and Scott (1976)
$1.5\frac{f_{pi}}{f_{ci}}d_s - 117$	Zia and Moustafa (1977)
$0.33f_{pi}d_b\sqrt{\frac{3}{f'_{ci}}}\frac{f_{pi}}{20.7}d_s\sqrt{\frac{20.7}{f_{ci}}}$	Mitchell et al. (1993)
$\left[\frac{4f_{pi}}{f_{ci}}d_s\right]$ - 127	Lane (1998)
$\alpha\frac{f_{pi}}{\sqrt{f_{ci}}}d_s$	Barnes et al. (2003)
$\frac{2.5A_{ps}f_{pi}}{P_t^{2/3}}$	Martí-Vargas et al. (2006)
$0.045\frac{f_{pi}(25.4 - d_s)^2}{\sqrt{f_{ci}}}$	Kose and Burkett (2007)
$\frac{315}{\sqrt{f_{ci}}}d_s \geqslant 40d_s$	Ramirez and Russell (2008)
$e^{\alpha + \beta d_s + \gamma f_{pi} + \delta f_{ci}}$	Pellegrino et al. (2015)
$25.7\left(\frac{f_{pi}}{\sqrt{f_{ci}}}d_s\right)^{0.55}$	Ramirez-Garcia et al. (2016)

Table 2
Parameters considered in the different equations for L_t.

Codes	Effective prestress	Diameter of strand	Compressive strength of concrete at transfer	Bond stress/ condition	Type of tendon	Prestress releasing method
AASHTO (2012)	✗	✓	✗	✗	✗	✗
AS 3600 (2009)						
CSA (2004)						
IS 1343 (2012)						
ACI 318 (2014)	✓	✓	✗	✗	✗	✗
BS 8110 (1997)	✗	✓	✓	✗	✓	✗
EN 2 (2004)/IRC 112 (2011)	✓	✓	✓	✓	✓	✓
fib-MC (2010)						

✓ Considered in the codes
✗ Not considered in the codes

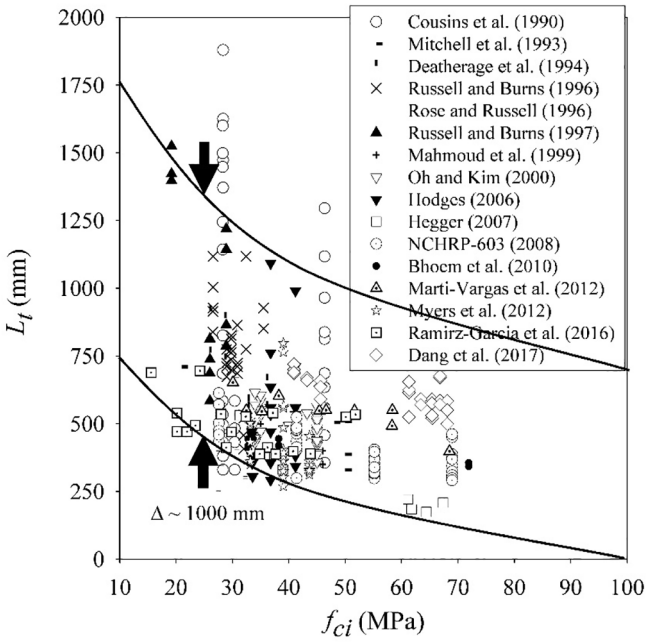

Fig. 3. Reported L_t as a function of f_{ci}.

from literature were collected and plotted as a function of f_c (see Fig. 3) [16,22,27–30,32,40,44,48–50]. This shows that L_t decreases as f_{ci} increases; therefore, f_{ci} must be included as a variable in the design equations to determine L_t. Also, Fig. 3 shows a large scatter (say, about 1000 mm as indicated by the gap between two boundary curves) among the values reported by different studies for the PTC systems. The data from literature contain values of L_t for different types of strand (coated strands and FRP strands) and releasing methods (gradual/sudden). Among these, the work by Cousins et al. (1990), Deatherage et al. (1994) and Russell and Burns (1997), Mahmoud et al. (1999), Oh and Kim (2000), Hodges (2006), Bhoem et al. (2010), and Myers et al. (2012) used sudden prestress release using flame cut, which resulted in longer L_t (varying from 400 to 1500 mm). This difference in L_t could be seen in the range of f_{ci} about 30–40 MPa. Some of these studies used different types of strands with coatings and different material composition, which could also significantly affect the L_t. Therefore, the values of L_t obtained from the various studies for the same f_{ci} are not comparable. Hence, the effect of f_{ci} could not be deduced/modelled using these data. Ramirez–Garcia et al. (2016) proposed an equation to calculate the L_t based on their experimental data and reported data from the literature. It was observed that there is significant scatter between the reported experimental and literature data. In such case, proposing an equation based on all these data may not be rational. Therefore, in this study, the values of L_t only for uncoated steel strands based on gradual release method were considered to compare with the experimental results.

2. Research significance

It is found that significant discrepancies exist among the design L_t equations in the various codes and literature. Some codes provide empirical formulations to estimate L_t as a function of only the properties of strands and do not consider that of concrete. This paper highlights the influence of f_{ci} on L_t. Also, the influence of seemingly simple, but complex test procedures on the determined L_t and its scatter are explained. Based on the experimental results with various strength grade concretes, a bi–linear model for L_t as a function of the properties of both strand and concrete is developed. It is anticipated that the proposed equation would be incorporated in the design codes to achieve more rational estimates of L_t, and hence, more refined structural designs for the end zone reinforcements of PTC members.

3. Experimental programme

The important information of the experimental programme is briefly presented for ready reference. Three prism specimens, each for

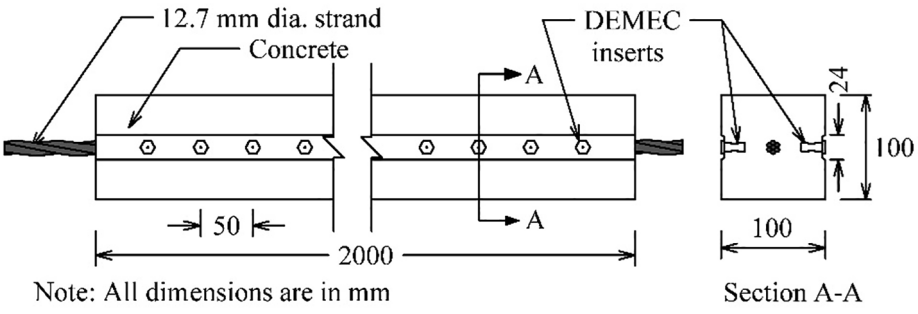

Fig. 4. The diagram of the prism specimen.

f_{ci} equal to 23, 28, 36, or 43 MPa were cast and tested for measuring L_t. Fig. 4 shows the diagram of a prism specimen [(100 × 100 × 2000) mm size] with a concentrically embedded prestressing strand in concrete. Also, companion cube specimens [(100 × 100 × 100) mm size] were cast and cured simultaneously, to determine f_{ci} under compression test.

3.1. Materials

Seven-wire, prestressing steel strands with a nominal diameter of 12.7 mm, pitch of 184 mm, a modulus of elasticity of 196 GPa, and an ultimate tensile strength of ≈1840 MPa were used in this study. Table 3 shows the chemical composition of the prestressing steel. The OPC 53S grade cement (finely ground; IS 269, 2015) was used to achieve the sufficient 3-day compressive strength (to transfer the prestress in 3 days) [51]. Polycarboxylate ether-based superplasticizer was used to achieve the desired workability (say, slump of 100 ± 20 mm) for the concrete. As per IS 1343 (2012), the grades of concrete recommended for PTC construction are M35 and above. Hence, in this study, the concrete mixes with an average f_{ci} of 23, 28, 36, and 43 MPa (these represent values close to those of grades M35, M45, M55, and M65, respectively) were used and the mix details are provided in Table 4. The moduli of elasticity of the concretes at 28 days for f_{ci} = 23, 28, 36, and 43 MPa were 30, 33, 35, 39 GPa, respectively.

3.2. Preparation of prism specimens

Fig. 5 shows the setup with the prestressing bed and L_t specimen. The self-equilibrating prestressing bed consisted of a hollow steel section with two end brackets. Fig. 5 also shows the close-up of the end anchorages and the stress adjusting system (SAS). Further details on this is provided in Mohandoss et al. (2018) [3] . The L_t specimens were prepared in three stages as follows.

3.2.1. Stage 1: Prestressing the strand

A 5.5 m long seven–wire strand was inserted in the through-holes of the end brackets of the steel prestressing bed (Fig. 5). Then, an initial prestress of about 0.75 f_{pk} was applied. At the jacking end (JE), a hydraulic jack (300 kN capacity), was placed to apply the stress. Steel chair, wedges and barrels, and load cell were also kept to, activate the stress reaction, lock the stress, and monitor the load applied, respectively. At the releasing end (RE), the stress adjusting system (SAS) and wedges and barrels were placed to lock, adjust, and gradually release the applied stress.

3.2.2. Stage 2: Placement of concrete and brass inserts

After stressing the strand, a custom-designed PVC mould was placed around the strand (on the prestressing bed) to place the concrete. Hexagonal brass inserts with bolt/head and nut/base were designed and fabricated. These were affixed to acrylic strips with pre-defined holes (50 mm c/c spacing) for accurate spacing and alignment. These strips with brass inserts were then placed along the center line of the two opposite, vertical surfaces on the inside faces of the PVC mould. It should be noted that achieving uniform compaction of concrete along the strand was crucial for the study. To achieve this, concrete in the PVC mould was placed in a single layer of 100 mm height and compacted uniformly (25 tampings for every 100 mm length). After 24 hrs, the L_t specimen and the accompanying cube specimens were demoulded. Then, the acrylic strips were removed from the concrete surface (by unscrewing the bolt/head of the inserts). Then, the bolt/head of the inserts was threaded again to the nut/base – to facilitate DEMEC gauge measurements.

Table 4
Concrete mix details.

Ingredients	Values of f_{ci} (MPa)			
	f_{ci}23	f_{ci}28	f_{ci}36	f_{ci}43
Cement (kg/m^3)	380	380	420	420
Water – cement ratio	0.50	0.45	0.40	0.35
10 mm aggregate (kg/m^3)	432	436	428	433
20 mm aggregate (kg/m^3)	648	655	641	649
Fine aggregate (kg/m^3)	750	758	743	752
Polycarboxylate ether-based Superplasticizer (% bwoc)	0.8	0.3	0.6	0.5

3.2.3. Stage 3: Curing of concrete and transferring of prestress

The specimens were cured (by covering with wet burlap and plastic sheet) until 3 days or when the concrete attained about 60% of the target compressive strength, whichever was earlier. After sufficient curing the prestress was gradually transferred from the strand to the concrete using the SAS system as shown in Fig. 5.

3.3. Strain measurements and estimation of L_t

The L_t can be estimated using the strain on the strand surface or concrete surface. Unlike in unstressed reinforcing bars, the accurate measurement of stretched strand is difficult. This is because placing of a strain gauge on the strand surface could locally affect the S–C bond [52] and the gauge would snap during stretching. Also, Russell and Burns (1997) suggested to use DEMEC measurements on concrete surface to minimize manual errors. Hence, in this study, the strains measured on the concrete surface using 150 mm gauge length was used to estimate the L_t. The measured data was smoothened by averaging the strain data over three consecutive/overlapping 150 mm gauge readings. Then, the average maximum strain (AMS), as defined by Russell and Burns (1997), was computed by averaging all the strain measurements on the plateau. The detailed description on this could be found in Mohandoss et al. (2018). The L_t is defined as the distance from the end of the member to the point with average strain equal to the 95% of AMS. In this way, L_t at both ends of the specimen was calculated and the average of the two values was defined as the L_t of the specimen.

4. Results and discussions

4.1. Challenges in strain measurements

Strain measurements on concrete surfaces are heavily dependent on the type of gauges used and bond conditions, especially for long-term measurements. In this study, initially DEMEC discs were glued onto the concrete surface using acrylic based adhesive. It was observed that this glue could not provide sufficient bond between these discs and concrete – probably due to the moisture curing practices and/or smooth/machined surfaces of the discs. Also, the force exerted by the technician while placing the gauge onto the DEMEC disc could also lead to debonding. To avoid such issues, custom–made brass inserts were used to obtain quality data, especially for long–term measurements. A brass insert was profiled with a 6 mm wide groove to ensure adequate bond/grip [3].

For a comparative study, the strain measurements were taken using

Table 3
Chemical composition of prestressing steel.

Element	C	Si	Mn	P	Cr	Ni	Al	Co	Cu	S	Fe
Conc. (%)	0.72	0.21	0.94	0.02	0.27	0.02	0.01	0.02	0.02	0.002	97.8

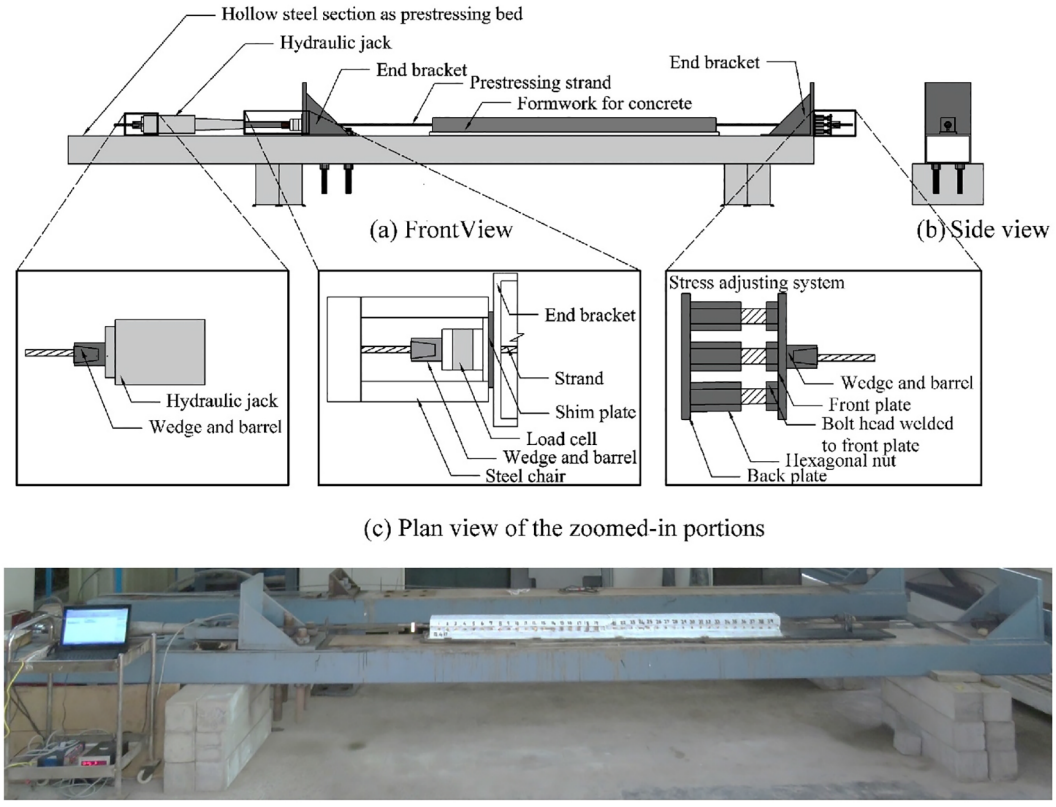

Fig. 5. Sketches and photograph of prestressing bed with PTC specimen.

discs and inserts placed on the same surface of a L_t specimen. As shown in the top-right corner of Fig. 6, inserts were placed along the mid-depth on opposite side faces of the specimen (indicated as I and I′) and the discs were placed adjacent to the inserts (indicated as D and D′); and companion readings were taken. The two curves with filled and unfilled markers in Fig. 6 indicate that discs can significantly underestimate the strain measurements, when above 300 με. For example, at about 600 mm from the end of the member, the strain values obtained using inserts and discs were about 550 and 400 με, respectively – indicating a reduction of about 25%. The strain values calculated using Hooke's law, applied stress, and the measured elastic modulus of concrete were closer to the strains obtained using the inserts than that using the discs. Hence, the inserts were used in the remainder of this study.

4.2. Influence of f_{ci} on L_t

Table 5 presents the f_{ci}, f_{pe} at transfer, and measured L_t (denoted as $L_{t,\ measured}$) at both jacking and releasing ends of all the specimens. Fig. 7 shows the smoothened variation of strain, $(\varepsilon'_c)_x$, along the length of the specimens. The values of $L_{t,\ measured}$ at both the jacking and releasing ends were found to be similar as gradual stress releasing method was adapted in this study [53]. At transfer, the strain on the concrete surface increased along the length of the member from the end and became constant. The average maximum strain (AMS), as defined by Russell and Burns (1997), was computed by averaging all the strain measurements on the plateau. The L_t is defined as the distance from the end of the member to the point with average strain equal to the 95% of AMS. The average strain for all the strengths of concrete at transfer was about 500–530 με. As the stress is transferred from the strand to concrete at 3 days, the strain variations between the different specimens could be in the range of 5 to 20 microstrains, which could be not exactly captured by DEMEC gauge. The average L_t for specimens with f_{ci} = 23, 28, 36, and 43 MPa strength concretes were 580, 565, 465, and 385 mm, respectively, with coefficients of variations of about 2 to 10%, which is reasonable. Also, it was observed that the scatter in the values of L_t was less with increasing strength of concrete.

Fig. 8(a) indicates the variation of L_t with compressive strength of concrete at transfer. Then the measured values of L_t were normalized w.r.t f_{pe} and d_s to model L_t as a function of only f_{ci}. This was based on the assumptions that L_t varies linearly with respect to f_{pe} and d_s alone. As L_t decreased with increasing L_t, to capture the effect of f_{ci}, a scatter plot between the inverse of f_{ci} and normalized $L_{t,\ measured}$ w.r.t f_{pe} and d_s was developed (see Fig. 8(b)). From the plot, it was observed that the trend of L_t as a function of $1/f_{ci}$ was bi-linear. For a lower f_{ci} (23 and 28 MPa), L_t did not decrease significantly with increase in f_{ci}. However, for concrete with strength higher than 28 MPa, significant reduction (say, upto 32%) in L_t was observed. Therefore, a bilinear model was

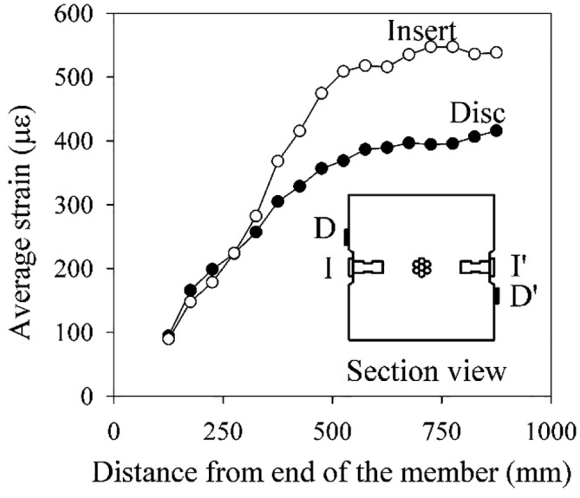

Fig. 6. Difference in strains from inserts and discs (Inset shows section view).

Table 5
Values of transmission length for different values of compressive strength of concrete at transfer.

Specimen ID	f_{ci} (MPa)	f_{pe} (MPa)	$L_{t,\ measured}$ (mm) JE	RE	Avg.	$L_{t,\ avg.}$ (mm)	Std. dev. (mm)
f_{ci}23 – 1	23.5	1270	630	565	598	580	32
f_{ci}23 – 2	22.8	1189	520	570	545		
f_{ci}23 – 3	22.1	1230	625	580	600		
f_{ci}28 – 1	28.0	1179	550	570	560	565	17
f_{ci}28 – 2	29.0	1209	540	560	550		
f_{ci}28 – 3	28.7	1220	565	600	585		
f_{ci}36 – 1	37.1	1148	480	500	490	465	28
f_{ci}36 – 2	36.0	1179	460	470	465		
f_{ci}36 – 3	36.8	1120	425	445	435		
f_{ci}43 – 1	43.4	1169	385	370	375	385	9
f_{ci}43 – 2	42.6	1189	385	405	395		
f_{ci}43 – 3	43.7	1108	400	375	390		

developed as given in Eqs. (1) and (2).

For $f_{c\ i} \leq 28$ MPa

$$L_t = f_{pe} d_s \left(0.028 + \frac{0.24}{f_{ci}}\right) \quad (1)$$

For $28 \leq f_{c\ i} \leq 43$ MPa

$$L_t = f_{pe} d_s \left(0.0036 + \frac{0.94}{f_{ci}}\right) \quad (2)$$

Fig. 9 shows the correlation between the L_t estimated using Eqs. (1) and (2) and $L_{t,\ measured}$. Many data points lie between the two dashed-lines (one standard deviation away from the average line) indicating reasonable prediction. Also, the mean absolute percent error (MAPE) of the model is found to be 3%, – indicating reasonable prediction accuracy.

4.3. Comparison of L_t obtained from the proposed model and various codes

Fig. 10 shows the comparison of L_t obtained from the proposed models and various codes (considering f_{ci}). The straight lines indicate the L_t obtained using AASHTO, AS, ACI, CSA, and IS codes (i.e., not a function of f_{ci}). However, L_t curves based on EN 2 (2004), *fib*–MC (2010), and the proposed model show a downward trend as the concrete strength increases. In general, PTC members will use concrete with f_{ci} more than 20 MPa. Considering this, Fig. 10 indicates that all the codes, except IS 1343 (2012), and the proposed model overestimate the L_t. Overestimation is not a conservative approach for design of stirrups for bursting stress near the ends and this is explained in the following section. Hence, a rational approach in estimating L_t is required based on f_{ci}. Also, concrete strength achieved could be lower than the desired or target strength due to poor construction materials and practices, which could result in longer L_t, which could reduce the available shear stress in the transmission zone.

The values of L_t based on proposed model were compared with values of L_t from the literature (see Fig. 11). Certain individual data points from Mitchell et al. (1993), Hegger (2007), NCHRP-603 (2008), and Ramirez-Garcia et al. (2016) studies matched with the proposed model. This could be due to gradual releasing method used in those studies, as adapted in the present work. Russell and Burns et al. (1996) adapted a combination of gradual and sudden release methods and resulted slightly longer than the measured L_t. All these studies determined the L_t based on the strain measurement on the concrete surface except Martí-Vargas et al. (2012). Martí-Vargas et al. (2012) determined the L_t by measuring the effective force on the strand using AMA systems, which is a virtual part of the specimen, whose stiffness would be more than the concrete part that was replaced. In addition, specimen size used in different studies are different which could also affect the measurement of L_t.

There are some scatters due to the difference in the geometry and materials considered in the various studies. Therefore, the values of L_t obtained from the various studies for the same f_{ci} are not comparable. Ramirez-Garcia et al. (2016) reported that L_t is not varied significantly when the f_{ci} was greater than 34 MPa. Based on their work, this maybe applicable for 15.2 mm strands but not for 12.7 mm strand as f_{ci} greater than 35 MPa was not considered for 12.7 mm strands. However, the reported literature data and proposed model show a significant

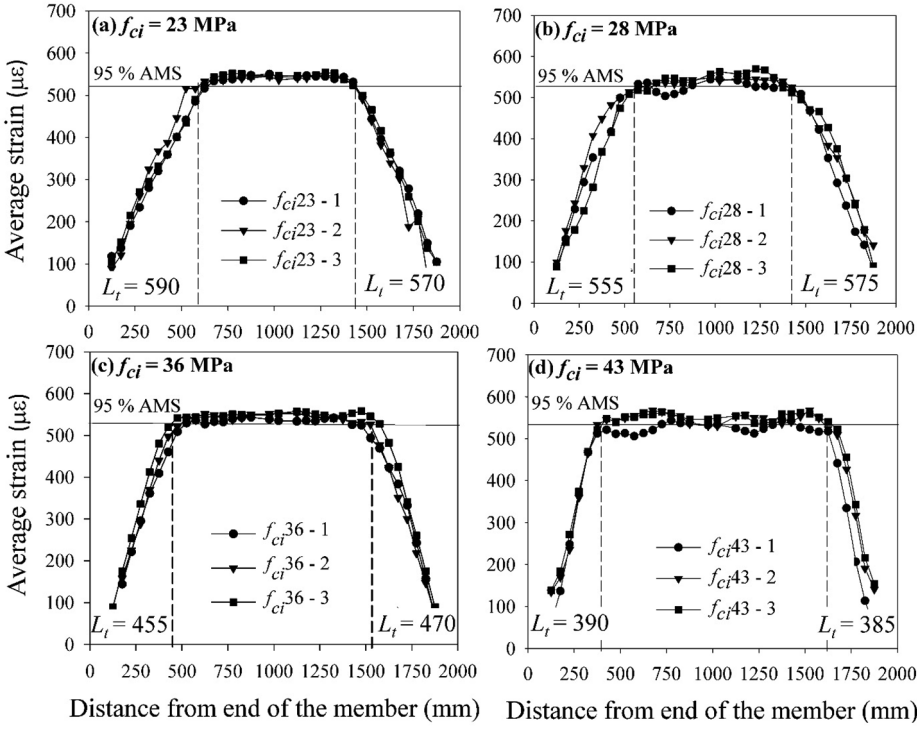

Fig. 7. Variations of strains on the concrete surfaces for different f_{ci}.

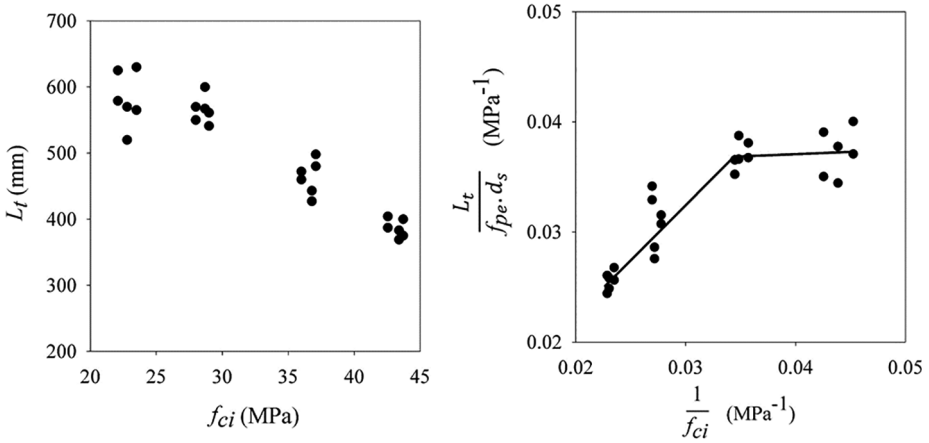

(a) L_t as a function of f_{ci} (b) Modelling of L_t as a function of f_{ci}

Fig. 8. Variation of L_t with the compressive strength of concrete at transfer.

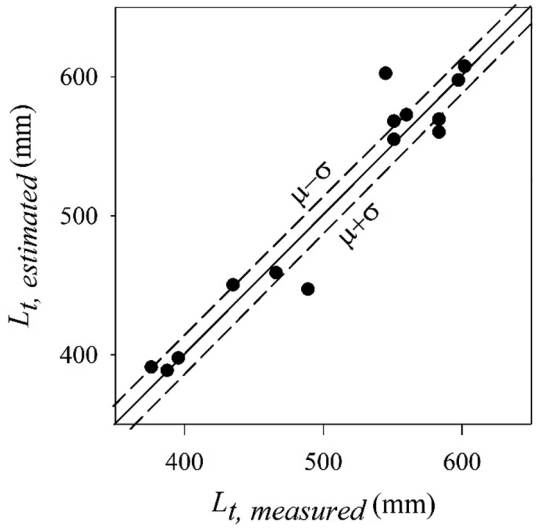

Fig. 9. Correlation between $L_{t,\ estimated}$ and $L_{t,\ measured}$.

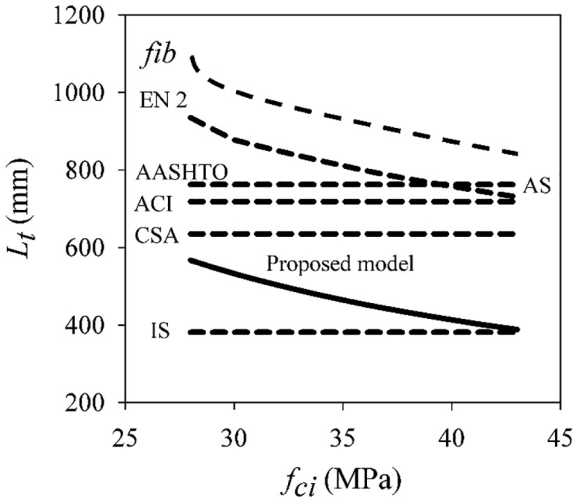

Fig. 10. Comparison of L_t models as function of f_{ci}.

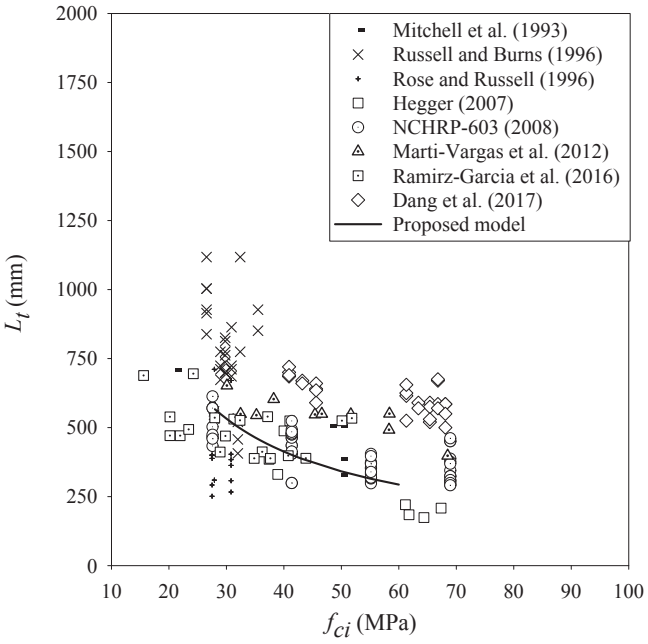

Fig. 11. Comparison of proposed model with L_t from literature.

reduction in L_t for f_{ci} greater than 34 MPa. This indicates that f_{ci} greater than 35 MPa has an effect on L_t, as it depends on the bond between the strand and concrete.

4.4. Effect of overestimation of L_t on the design of stirrups for bursting stresses

In the transmission zone of the PTC beams, transverse reinforcement is necessary to prevent the concrete cracking due to large radially outward stresses. The crack occurs when the maximum stresses exceed the tensile strength of the concrete. At the end of the member, the transverse tensile stress is maximum and gradually gets reduced along the length in the transmission zone [54]. However, for the design of end reinforcement, this transverse tensile stress was approximated as a linear variation over half the L_t [55]. The transverse tensile force and area of the vertical reinforcement are computed as follows using Eqs.

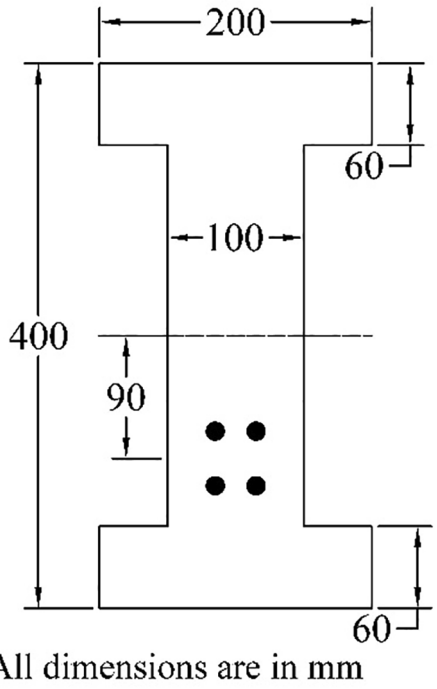

Fig. 12. Cross section of a simple girder.

(3) and (4).

$$F_{bat} = \frac{1}{2} f_{v(max)} \frac{L_t}{2b_w} \quad (3)$$

$$A_{sv} = \left[\frac{2.5M}{f_s D} \right] \quad (4)$$

These tensile stresses are dependent on the prestress level, rate of prestress transfer along the length, etc., which influence the L_t. As an example study, the tensile stress (f_t) distribution at the level of the centroid of strands along the length of a PTC beam was investigated to determine the effect of overestimation of L_t on the transverse tensile stress at the end of the member. Fig. 12 shows the cross section of the beam considered for the study.

Fig. 13(a) presents the tensile stress distribution in the transmission zone for different L_t ranging from 300 to 1500 mm. At the end of the member, the tensile stress was maximum and it gradually decreased to zero at the end of transmission zone. In general, overestimation of transmission length is considered as a safe design. Therefore, importance was not given to this aspect. The authors' previous paper (Mohandoss et al. (2018)) addressed the significance of underestimation of transmission length and its effect on the shear capacity of the members. This paper attempted to highlight only the case with overestimation of L_t. Fig. 13(b) shows the maximum tensile stress as a function of the L_t for the f_{ci} = 42 MPa. It indicates that if the L_t is overestimated, then the maximum tensile stress is under estimated and vice versa. As a consequence, this reduces the area and increases spacing of the stirrups in the transmission zone, resulting in less shear reinforcement. In this case, it could result in bursting and/or cracking at prestress transfer. Hence, it is important not to overestimate the transmission length beyond certain limit. According to the current study, an overestimation up to 30% seems safe. This scenario could become worse, if the strength of concrete is lower than 42 MPa. This is critical, especially in narrow web pretensioned beams/girders, where the strands would be closely placed and congested [56]. Therefore, the overestimation of L_t beyond 30% of the values from tests should be avoided while designing PTC members.

5. Summary and conclusions

The transmission lengths (L_t) for pre–tensioned concrete (PTC) members for several values of the compressive strength of concrete at transfer (f_{ci}), were experimentally obtained from twelve specimens. Based on this experimental data, a bi–linear model was developed for determination of L_t as a function of f_{ci} (Eqs. (1) and (2)). The values from the proposed model were compared with those obtained from several codes. Also, an example study was done to understand the significance of the overestimation of L_t. The following conclusions were drawn from the present study.

- The compressive strength of concrete at transfer has a significant influence on L_t. When f_{ci} increased from 23 to 43 MPa, the possible range in practice, the values of L_t decreased from about 600 to 400 mm (33% reduction). Also, the scatter in the values of L_t was less with increasing strength of concrete.
- For the range of concrete compressive strength at transfer used in PTC systems, the AASHTO, ACI, AS, CSA, EN and *fib* codes overestimate the values of L_t, when compared with those estimated using the proposed model. Only the Indian standard underestimates the value of L_t.
- From the case study, it was observed that the overestimation of L_t is not advisable for the design of the transmission zone reinforcement required for the bursting stresses. Hence, the proposed model that considers the compressive strength of concrete at transfer to

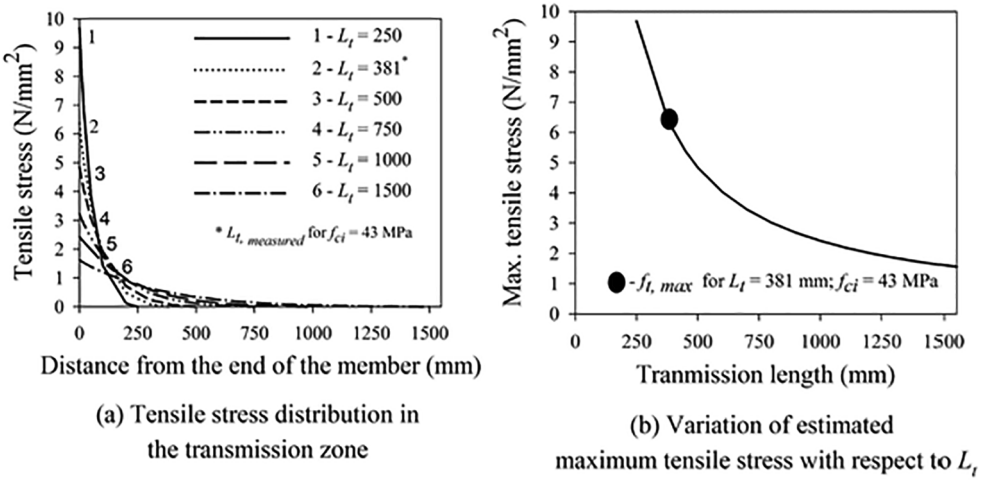

Fig. 13. Bursting tensile stresses in the transmission zone.

estimate L_t precisely is expected to provide a more rational design of the transmission zone reinforcement.

Declaration of Competing Interest

The authors declare that they have no known competing financial interests or personal relationships that could have appeared to influence the work reported in this paper.

Acknowledgements

The authors acknowledge the financial support through the 'Fund for Improvement of Science & Technology Infrastructure (FIST)' Grant ETII-054/2012 from the Department of Science and Technology (DST), and other financial support from the Ministry of Human Resource Development (MHRD), Govt. of India, through the Department of Civil Engineering, Indian Institute of Technology Madras (IITM), Chennai. The authors express their gratitude to Prof. Ravindra Gettu, president, RILEM for his valuable feedback and suggestions on this research work. The authors also acknowledge the assistance from the laboratory staff and students in the Construction Materials Research Laboratory at IITM.

REFERENCES

[1] Barnes RW, Grove JW, Burns NH. Experimental assessment of factors affecting transfer length. ACI Struct. J. 2003;100(6):740–8.
[2] Mohandoss P, Pillai RG, Sengupta AK. Comparison of prediction models for transmission length and shear capacity of pre-tensioned concrete systems. In: 4th Asian Conference on Ecstasy in Concrete (ACECON), Kolkata, India; 2015. p. 183–193.
[3] Mohandoss P, Pillai RG, Sengupta AK. Transmission length of pretensioned concrete systems – comparison of codes and test data. Mag. Concr. Res. 2018. https://doi.org/10.1680/jmacr.17.00553.
[4] Janney JR. Nature of bond in pre-tensioned prestressed concrete. J. Am. Concr. Inst. 1954;25(9):717–36.
[5] Hanson NW, Kaar PH. Transmission length of pretensioned prestressed beams. J. Am. Concr. Inst. 1959;55(51):783–802.
[6] Hoyer E, Friedrirch E. Beitrag zur frage der haftspannung in eisinbeton bautellin. Beton Und Eiren 1939;50:717–36.
[7] American Association of State Highway and Transportation AASHTO, LFRD Bridge Design Specifications, interim revisions 6th ed., Washington, DC, 2012.
[8] American Concrete Institute ACI 318, Building Code Requirements for Reinforced Concrete. American Concrete Institute, Detroit, MI, USA, 2014.
[9] Australian Standard AS 3600, Concrete Structures, Standards Australia Limited, Sydney, NSW, Australia, 2009.
[10] Canadian Standards Association CSA A23.3, Design of Concrete Structures, Mississauga, Canada, 2004.
[11] European standard EN 2, Design of Concrete Structures – Part 1-2: General Rules for Buildings, Brussels, Belgium, 2004.
[12] Indian Road Congress IRC 112, Code of Practice for Concrete Road Bridges, New Delhi, India, 2011.
[13] International Federation for Structural Concrete (fib), Model Code for Concrete Structures, fib bulletin No. 55, Lausanne, Switzerland, 2010.
[14] Bureau of Indian Standards IS 1343, Prestressed Concrete – Code of Practice, New Delhi, India, 2012.
[15] Martin BLD, Scott NL. Development of prestressing strand in pretensioned members. Proc. ACI J. 1976;73(8):453–6.
[16] Cousins TE, Johnston DW, Zia P. Development length of epoxy-coated prestressing strand. ACI Mater. J. 1990;87(4):309–18.
[17] Belhadj A, Bahai H. Friction–slip: an efficient energy dissipating mechanism for suddenly released prestressing bars. Eng. Struct. 2001;23:934–44.
[18] Moon DY, Zi G, Kim J, Lee S, Kim G. On strain change of prestressing strand during detensioning procedures. Eng. Struct. 2010;32:2570–8.
[19] Rose DR, Russell BW. Investigation of standardized tests to measure the bond performance. PCI J. 1997;44(4):56–80.
[20] Russel BW, Burns NH. Measurement of transfer lengths on pretensioned concrete elements. J Struct Eng 1997;12(3):541–9.
[21] Zia P, Mostafa T. Development length of prestressing strands. PCI J. 1997;22(5):54–65.
[22] Mitchell D, Cook WD, Khan AA. Influence of high strength concrete on transfer and development length of pretensioning Strand. PCI J. 1993;38(3):52–66.
[23] S. Lane, A New Development Length Equation for Pretensioned Strands in Bridge Beams and Piles, Mclean, VA, 1998.
[24] Martí-Vargas JR, Serna-Ros P, Fernandez-Prada MA, Miguel-Sosa PF. Test method for determination of the transmission and anchorage lengths in prestressed reinforcement. Mag. Concr. Res. 2006;58(1):21–9.
[25] Martí-Vargas JR, Serna-Ros P, Navarro-Gregori J, Pallarés L. Bond of 13 mm prestressing steel strands in pretensioned concrete members. Eng. Struct. 2012;41:403–12.
[26] Kose MM, Burkett WR. Formulations of new development length equation for 0.6 in. prestressing strand. PCI J. 2005;September–October:96–105.
[27] Ramirez J, Russell B. Transfer, development, and splice length for strand/reinforcement in high-strength concrete. NCHRP (National Cooperative Highway Research Program) report 603. Transportation Research Board, Washington, CS; 2008.
[28] Oh BH, Kim ES. Realistic evaluation of transfer lengths in pretensioned, prestressed concrete members. ACI Struct. J. 2000;97(6):821–30.
[29] Bhoem KM, Barnes RW, Schindler AK. Performance of self-consolidating concrete in prestressed girders highway research center. AL: Harbert Engineering Center Auburn University, The Alabama Department of transportation; 2010.
[30] Myers JJ, Volz JS, Sells E, Porterfield K, Looney T, Tucker B. Self-Consolidating Concrete (SCC) for Infrastructure Elements: Report B-bond, Transfer Length, and Development Length of Prestressing Strand. Rolla, MO: Missouri University of Science and Technology; 2012.
[31] Ramirez-Garcia AT, Dang CN, Hale WM, Martí-Vargas JR. A higher-order equation for modeling strand in pretensioned concrete beams. Eng. Struct. 2017;131:345–61.
[32] Russell BW, Burns NH. Measured transfer length of 0.5 and 0.6 in. strands in pretensioned concrete. PCI J. 1996;September–October:44–65.
[33] Kim JK, Yang JM, Yim HJ. Experimental evaluation of transfer length in pretensioned concrete beams using 2400 MPa prestressed strands. J Struct Eng 2016;142(11). 04016088-1-04016088-10.
[34] Vázquez-Herrero C, Martínez-Lage I, Martínez-Abella F. Transfer length in pretensioned prestressed concrete structures composed of high performance lightweight and normal – weight concrete. Eng. Struct. 2013;56:983–92.
[35] Kaar PH, Lafraugh RW, Mass MA. Influence of concrete strength on strand transfer length. In: Ninth Annual Convention of the Prestressed Concrete Institute; 1963. p. 47–67.
[36] Bruce RN, Russell HG, Roller J, Martin BT. Feasibility evaluation of utilizing high-strength concrete in design and construction of highway bridge structures. Baton Rouge, LA: Louisiana Transportation Research Center; 1994.
[37] International Federation for Structural Concrete (fib), Bond of Reinforcement in Concrete–State of the art report fib bulletin No. 10, Lausanne, Switzerland, 2000.
[38] Dorsten V, Hunt FF, Preston HK. Epoxy coated seven-wire strand for prestressed concrete. PCI J. 1984;29(4):100–9.
[39] Roller JJ, Martin BT, Russell HG. Performance of prestressed high strength concrete bridge girders. PCI J. 1993;38(3):34–45.
[40] Mahmoud ZI, Rizkalla SH, Zaghloul ER. Transfer and development lengths of carbon fiber reinforced polymers prestressing reinforcement. ACI Struct. J. 1999;96(4):594–602.
[41] Caro LA, Martí-Vargas JR, Serna P. Time–dependent evolution of strand transfer length in pretensioned prestressed concrete members. Mech. Time-Depend. Mater. 2013;17(4):501–27.
[42] British Standard BS 8110-1, Structural Use of Concrete – Part 1: Code of Practice for Design and Construction, London, UK, 1997.
[43] Dang CN, Hale WM, Martí-Vargas JR. Assessment of transmission length of prestressing strands according to *fib* Model Code 2010. Eng. Struct. 2017;147(2017):425–33.
[44] Shahawy MA, Issa M, Batchelor B. Strand transfer lengths in full scale AASHTO prestressed concrete girders. PCI J. 1992;37(3):84–6.
[45] Deatherage JH, Burdette EG, Chew CK. Development length and lateral spacing requirements of prestressing strand for prestressed concrete bridge girders. PCI J. 1994;39(1):70–83.
[46] Buckner CD. A review of strand development length for pretensioned. PCI J. 1995;40(2):84–105.
[47] Pellegrino C, Zanini MA, Faleschini F, Corain L. Predicting bond formulations for prestressed concrete elements. Eng. Struct. 2015;97:105–17.
[48] Ramirez-Garcia AT, Floyd RW, Hale WM, Martí-Vargas JR. Effect of concrete compressive strength on transfer length. Structures 2016;5:131–40.
[49] Hodges HT. Top Strand Effect and Evaluation of Effective Prestress in Prestressed Concrete Beams [research]. Blacksburg, VA: Virginia Polytechnic Institute and State University; 2006.
[50] Martí-Vargas JR, Serna P, Navarro-Gregori J, Bonet JL. Effects of concrete composition on transmission length of prestressing strands. Constr. Build. Mater. 2012;27:350–6.
[51] Bureau of Indian Standards IS 269, Ordinary Portland Cement – Specification, New Delhi, India, 2015.
[52] Park H, Din ZU, Cho J. Methodological aspects in measurement of strand transfer length in pretensioned concrete. ACI Struct. J. 2013;109(5):625–34.
[53] Benítez JM, Gálvez JC. Bond modelling of prestressed concrete during the prestressing force release. Mater. Struct. 2011;44:263–78.
[54] Krishnamurthy D. A method of determining the tensile stresses in the end zones of pretensioned beams. Indian Concr. J. 1971;45(7):286–697.
[55] Raju KN. Prestressed Concrete. fourth edition New Delhi, India: Tata McGraw Hill; 2011.
[56] Tuan YC, Yehia AS, Jongpitaksseel N, Tadros KM. End zone reinforcement for pretensioned concrete girders. PCI J 2004;49:1–16.